University of Texas at Austin

Senior Thesis

Multiphoton Lithography of Solid Protein Microstructures

Author: Rikki Garner

Supervisors: Dr. Eric Spivey, Dr. Jason Shear, and Dr. Vernita Gordon

In partial fulfillment of the requirements for graduation with the Dean's Scholars Honor's Degree in the Department of Physics.

May 08, 2013

Approved and recommended for acceptance as a senior thesis in partial fulfillment of the requirements for graduation with the Dean's Scholars Honor's Degree in the Department of Physics.

Dr. Eric Spivey, Department of Chemistry Research Adviser	Date
Dr. Jason Shear, Department of Chemistry Supervising Professor	Date
Dr. Vernita Gordon, Department of Physics Thesis Adviser	Date
Dr. Greg Sitz, Department of Physics Honor's Adviser	Date

Abstract

Multiphoton excitation is a process in which two or more photons are absorbed nearly simultaneously by a target molecule in order to excite an electron to a higher energy state. The Shear lab uses a mode-locked, Ti:S, femtosecond pulse laser system to initiate multiphoton excitation of a particular class of molecule called a photosensitizer, which undergoes a chemical reaction in the process of releasing energy. As the laser scans over a small volume of photosensitizer and protein in a buffer solution, the photosensitizer produces high-energy free radicals which diffuse and cause covalent crosslinking between the proteins to occur, creating a crosslinked solid structure within the focal volume. Because this reaction happens only within the focal volume, this method gives precision as small as hundreds of nanometers. These structures can be designed for many studies which require micron-scale precision, environmentally reactive properties (responses to temperature or pH changes), and biocompatibility. The two major projects are discussed in this thesis involve the effect of changing the constituents of the solution: the photosensitizer and the protein. In the first experiment, I synthesized a new type of photosensitizer. A benzophenone dimer was synthesized by running a reaction of 4-benzoylbenzoic acid, succinimidyl esterpowder and 1,3-diaminopropane, filtered using flash column chromatography, and identified using mass spectrometry and NMR analysis. While analysis showed we did create the molecule we intended, the benzophenone dimer was difficult to dissolve and could

not fabricate structures. In the second experiment, I used trypsin to hydrolyze bovine serum albumin over a wide range of digestion times, and used the digested fragments to fabricate structures. The structures were analyzed visually using SEM imaging and then through a swelling study, where fabrications were soaked in varying pH phosphate buffers and their dimensions were measured using a graphics software. The most notable result was that digested fragments were much less efficient at crosslinking, and were unable to form fine lines. However, there was no significant change in swelling, even at digestion times of up to twenty-four hours. Further studies on the quantization of the charge, size, and number of protein fragments from our digestion process are proposed.

Contents

1 Introduction

1.1 Multiphoton Lithography

1.1.1 Multiphoton Excitation

Multiphoton excitation (MPE) is a process in which two or more photons are absorbed nearly simultaneously by a target molecule in order to excite an electron to a higher energy state. This can be compared to single-photon excitation, in which a single, higher energy photon provides all of the energy required (Figure 1).

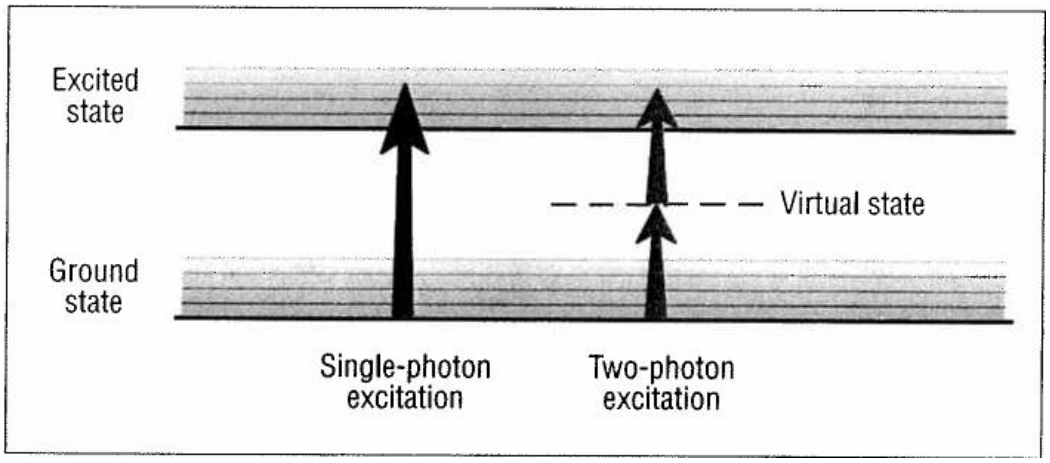

Figure 1: In single-photon excitation, the energy of the source photons must equal the energy gap between electronic levels. In this simplified representation, the same energy gap can be bridged through the nearly simultaneous absorption of two photons that each have twice the energy (half the wavelength) as the photon used for single-photon excitation. The multiphoton transition is often depicted as passing through one or more "virtual" states that persist for extremely brief periods according to uncertainty broadening of molecular energy levels [Shear, 1999].

There are two main advantages to using MPE. First, MPE allows for the use of lower energy photons, making it less likely to damage or photobleach the target material. Second, because excitation requires two or more photons to be absorbed at the same time, the probability of excitation is approximately dependent on the density of photons squared, rather than just the density of photons (Figure 2). This means the region of effective excitation is much smaller than with single-photon excitation (giving a smaller focal volume). Most of the literature on MPE is in reference to multiphoton excitation fluorescence microscopy, in which the small focal volume allows for greater optical-axis resolution of excited fluorophores. However, by exciting another light-reactive molecule called a photosensitizer, rather than a fluorophore, a photochemical reaction is induced inside the focal volume.

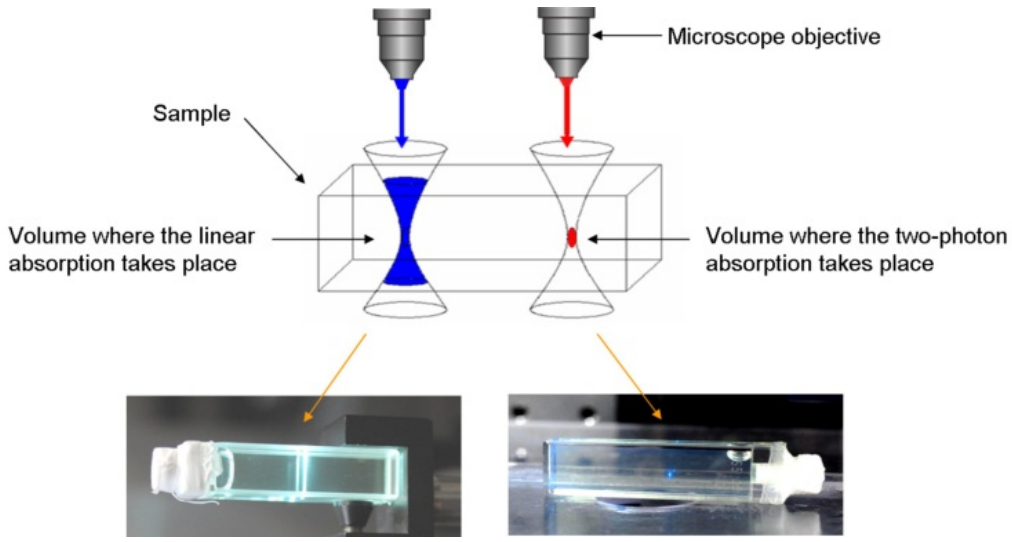

Figure 2: Multiphoton Excitation vs Single-photon Excitation [Dorkenoo, 2012]

1.1.2 Excitation of Photosensitizers and Crosslinking

While most substances can absorb and re-emit light, photosensitizers undergo efficient excitation to the triplet state, allowing them to remain excited and store energy for longer periods of time. Most photosensitizers will be composed of intramolecular bond structures which facilitate this, such as aromatic rings. To release energy, photosensitizers can a) re-emit light, b) undergo a chemical reaction and/or c) lose energy to heat and vibrations (we often see micron-scale explosions in the structures during fabrication). In the Shear lab, we use photosensitizers which release energy primarily under the second category. Most of these produce high-energy free radicals such as singlet oxygen, which diffuse and cause covalent crosslinking between the proteins to occur. Upon excitation from a high-intensity femtosecond laser pulse (necessary to concentrate enough photons into a small time and space), crosslinking will occur at a high enough density to fabricate solid structures. Photosensitizers will fabricate structures with many kinds of materials, including proteins, and the mechanical properties of the resulting fabrications will vary depending on which base materials are used. Some examples of the photosensitizers used in the lab are methylene blue (Figure 3) and rose bengal (Figure 4). Both of these structures have the characteristic aromatic ring structure found in many photosensitizers.

Methylene Blue:

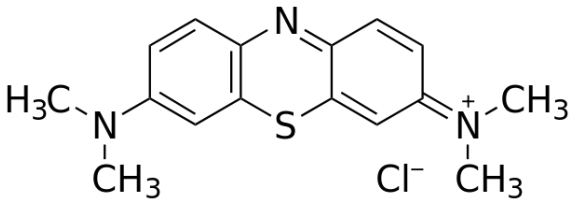

Figure 3: Methylene Blue Chemical Structure

Rose Bengal:

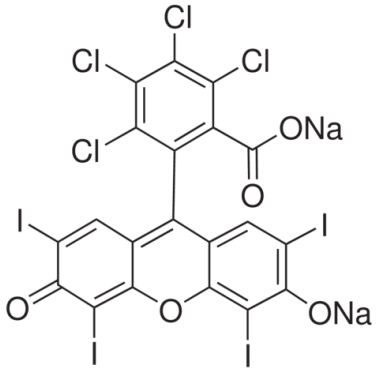

Figure 4: Rose Bengal Chemical Structure

1.1.3 Optimizing the Laser for High-Resolution Three-Dimensional Fabrication

One main advantage of the fabrication instrument in the Shear lab is its ability to quickly and efficiently fabricate complex, micron-scale shapes and designs. The laser is scanned over a digital micromirror device (DMD) that

acts as a dynamic, programmable reflectance mask. A DMD is an array of micro-mirrors which can be tilted in order to turn the reflecting light "on" or "off". These mirrors reflect the light through the objective and onto the sample for fabrication. The laser raster scans over the DMD (and thus over the sample) in two dimensions. Then the focal plane is shifted up by some amount relative to the sample and continues scanning. By using images created in Photoshop, Powerpoint or other graphics programs, we can display a series of images on the screen of the computer, and a program automatically fabricates that three dimensional object.

The following description can be found in Ritschdorff, et. al. [Ritschdorff, 2012] and is shown in Figure 5. Output from a mode-locked titanium:sapphire (Ti:S) oscillator (740 nm; Coherent Mira 900F pumped by a 10-W Coherent Verdi) is first passed through a telescoping lens set (TLS; fl = 5 cm) to establish a collimated beam. Light is then reflected from a scanbox containing a two-axis, galvanometer-driven scan mirror scavenged from a dismantled confocal microscope (Leica TCS-4D, Bensheim, Germany). The mirror is controlled by software written in LabView (National Instruments, Austin, TX) that provides independent control of the scan frequency, amplitude, phase, and waveform. The scanning beam is directed through lenses L1 (fl = 3.2 cm) and L2 (fl = 15.2 cm), then to L3 (fl = 15.2 cm), an arrangement that expands the beam and focuses it onto a DMD (from a partially dismantled Digital Light Processing (DLP) projector (BenQ, MP510)) to a spot size of $\approx$45 μm. Here, the optical axis of the beam is $\approx 90^{\circ}$ relative to the face of

the DMD, which results in a reflection angle of $\approx 20°$relative to the DMD face as a result of the 10° tilt of the micromirrors. The DMD is comprised of an 800 x 600 array of independently moving 16 μm x 16 μm aluminum mirrors (17 μm pixel pitch), corresponding to a total chip area of 13.6 mm x 10.2 mm.The beam is collimated by a tube lens (L4, fl = 15.2 cm) before being directed by a dichroic mirror (not shown) into a Zeiss Fluar microscope objective situated on a Zeiss Axiovert 135 inverted microscope. The objectives used are generally 1.3 NA or 1.35 NA oil immersion objectives. This setup can currently give fabrication resolution as low as hundreds of nm^3.

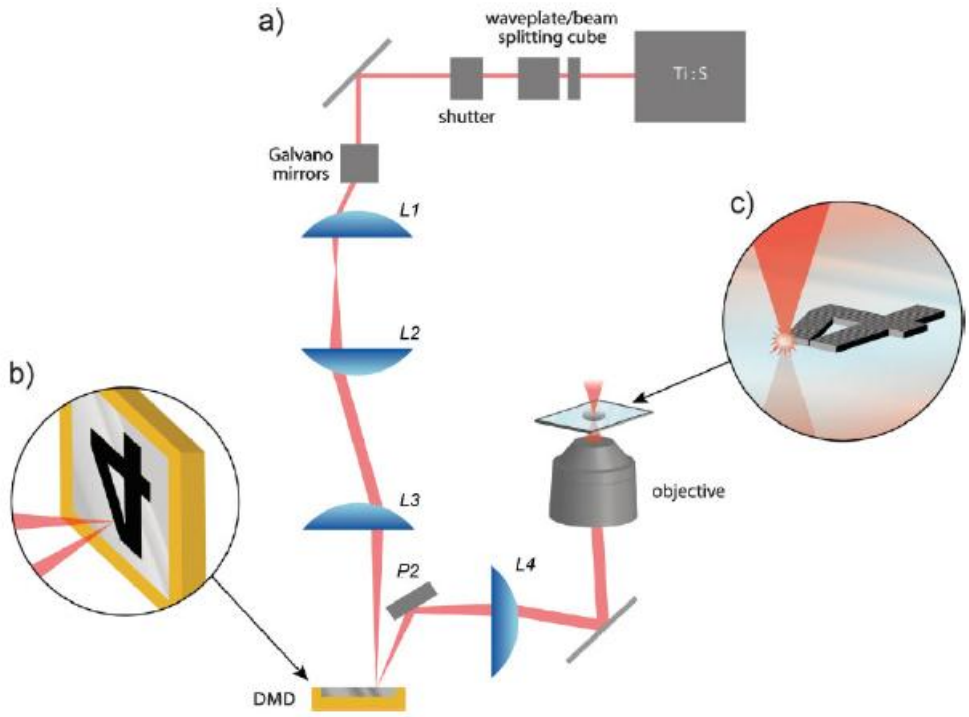

Figure 5: DMD-directed MPL. a) The output from a titanium sapphire (Ti:S) laser is attenuated using a waveplate and beam-splitting cube and is raster scanned using a pair of galvanodriven mirrors. Three relay lenses (L1, L2, and L3; focal lengths 2.5, 10.2, and 15.2 cm, respectively) direct the focused beam onto the face of the DMD. After reflection off the DMD the beam is guided by a periscope (P2) and is recollimated using a tube lens (L4, focal length 15.2 cm) before entering the microscope objective. b) Close-up showing interrogation of the DMD dynamic-mask using a scanned laser focus in which the region corresponding to the character 4 reflects the scanned laser light toward the microscope. c) A protein replica based on the mask image in (b) is fabricated in the microscope specimen plane [Nielson, 2009].

1.2 Motivations and Areas of Study

These structures can be designed for many studies which require micron-scale precision, environmentally reactive properties (responses to temperature or pH changes), and biocompatibility. These studies have tended to be focused on cell-surface interactions, microfluidics, and even combinations of the two. In particular, the biocompatible properties of these protein-based matrices as well as their adjustable mechanical properties make the microstructures ideal for applications such as trapping and organizing bacteria in order to study group behavior. Intricate, three-dimensional housing for cells, such as tunnels, grids, holes, and other traps were recently used to study quorum sensing among bacteria [Connell, 2010]. Furthermore, it has been shown that bacteria can be encapsulated in gelatin, which allows fabrication to be performed around free-floating bacteria without harming the cell [Connel, 2012]. Within the past year, the lab has been experimenting with fabrication in protogels, or water-based gels which are slowly dried into a glassy solid and dissolve easily in aqueous buffer. Once dissolved, there remain either free-floating structures or structures tethered by one end to the glass. Uses of these free or tethered structures are an active area of research, as microparticles of complex, arbitrary shapes could be of value in optimizing drug delivery or to be used as tracers [Spivey 2013].

One major drawback to the lab's method of fabrication is that it takes tens of minutes to fabricate structures just millimeters in size. Two methods that are being explored in order to combat this are synthesization of more

efficient photosensitizers and using PDMS molds to make hundreds of structures at a time. Fabrication scan speeds are highly dependent on how well the photosensitizer works, and how long the chemical reaction takes to run efficiently. One of my projects in this lab was to create a dimerized photosensitizer, in which two photosensitizers are attached by a hydrocarbon tether. This is done to potentially adjust the selection factors for multiphoton excitation of the molecule, ideally creating an absorption peak at the wavelengths used in the lab [Pitts, 2002]. By increasing the efficiency of this crosslinker at certain wavelengths, it is possible to increase the overall efficiency of the system. Another approach, molding, bypasses the scanning speed problem by creating replicas. An initial master structure is fabricated to the glass, and a mold is created from that master. Then, fabrication solution is poured into the master, sealed with glass, and then irradiated with UV light. This process is much more efficient for trying to mass-produce protein structures than it is for making many different unique structures.

2 A Novel Benzophenone Dimer

2.1 Motivations

One photosensitizer used in the Shear lab is benzophenone. Benzophenone photosensitizers are desirable because of three main properties: (1) they are chemically stable under ambient light, (2) are activated at 350-360 nanometers (which will not severely damage proteins), and (3) react preferentially

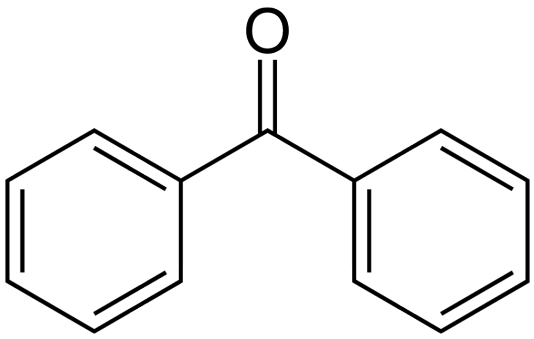

Figure 6: Benzophenone

with normally unreactive C-H bonds in the crosslinking material [Dorman, 1994]. For instance, benzophenones are traditionally used as probes in chemical reactions and as UV absorbers in plastic packaging to protect commercial products such as dyes and perfumes. However, benzophenones are disadvantageous due to their hydrophobicity. Shown in Figure 6, there again is the familiar aromatic ring structure. Shown in Figure 7 is its waxy appearance (signifying its hydrophobicity) at room temperature.

Figure 7: Macroscopic Benzophenone

When excited by UV radiation, one electron is shifted from the non-bonding sp^2 orbital on the oxygen to the π^* orbital on the carbonyl group. This leaves the benzophenone in its excited triplet state, in which the oxygen has an exposed electron. To stabilize itself, the benzophenone can then either undergo electron transfer from the carbon to the oxygen, leading to hydrogen abstraction from the target molecule to the benzophenone, or it can immediately undergo hydrogen abstraction. Both of these create other radical derivatives of the target molecule. These free radicals form C-C bonds, creating further crosslinking. These reactions can be seen in the chemical pathways shown in Figure 8.

It is possible to increase the efficiency of two-photon excitation of benzophenone at certain wavelengths by dimerizing it (connecting two benzophenones with a hydrocarbon tether). This enhances the crosslink bond density for a given laser power, which provides another photosensitizer option for

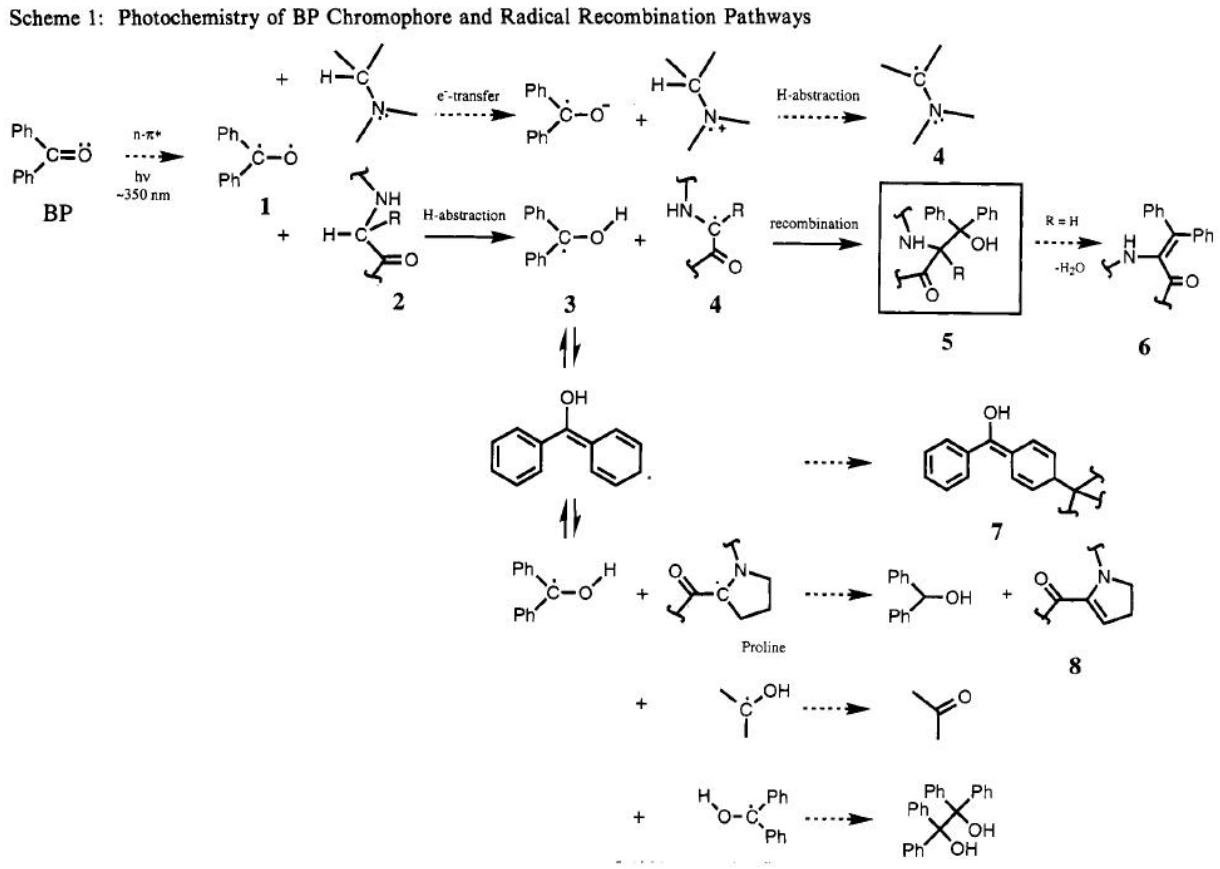

Figure 8: Benzophenone Radical Recombination Pathways [Dorman 1994]

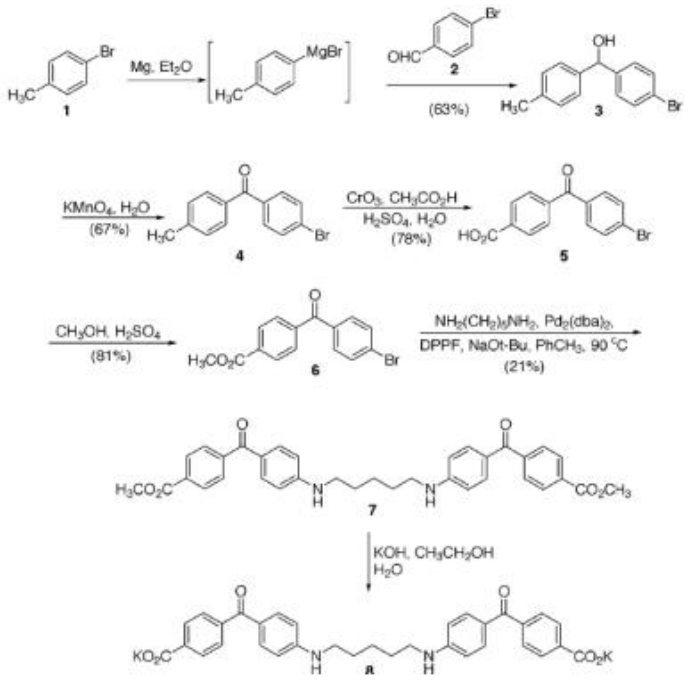

Figure 9: Previously Synthesized BenzophenoneDimer [Pitts, 2002]

fabrication. Benzophenones are specifically advantageous because they are transparent to visible wavelengths, do not act as a dye, and are less toxic to living systems than other photosensitizers used in the lab. The method used previously to create the dimer can be seen in Figure 9.

Noticing the complexity in deriving the previously-synthesized benzophenone dimer my advisor looked for a simpler, small-scale way to make this dimer. Seeing that we need two benzophenones with a hydrocarbon tether between them, it seemed that it could be energetically favorable to run a reaction between a compound containing a benzophenone and an amine group in solution. Searching the literature, he found an affordable benzophenone

succinimide powder. The theorized reaction goes as follows in Figures 10, 11 and 12:

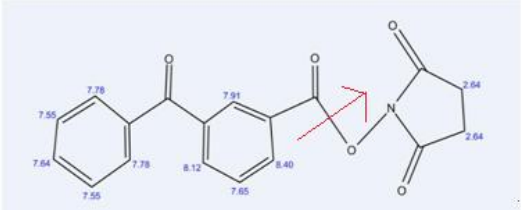

Figure 10: Benzophenone Succinimide

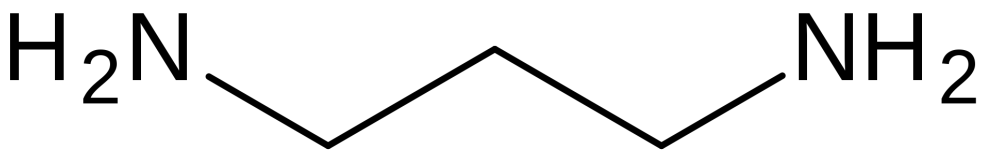

Figure 11: Diamino-propane

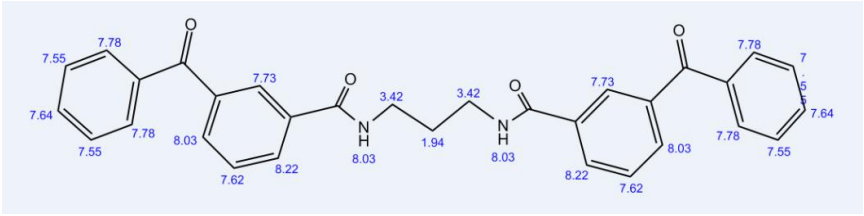

Figure 12: Benzophenone Dimer

2.2 Experimental Design

2.2.1 BP-SE/DAP Reaction

The reaction was to be run with a 2:1 mole fraction of BPSE to DAP with excess of BPSE. The expected yield was unknown at the time. I ran a reaction of 40mg of benzophenone succinimide (4-benzoylbenzoic acid, succinimidyl esterpowder B1577, Invitrogen) in 5 μL of 1,3-diaminopropane 94% (112352500, Acros Organics) via a magnetic stirring plate overnight ($\sim$24 hours).

2.2.2 Flash Column Liquid Chromatography

Column Chromatography is a method used to separate out constituents of a solution. The basic idea behind the method is to run the sample through a filter using different solvents, each of which dissolve different constituents preferentially. By collecting the products of the filter in 5mL samples in tubes over time, further studies can be performed to group the samples accordingly.

Key Terminology:

"analyte" = target compound

"adsorbant" = silica, which draws analyte to its surface

"eluent" = solvent

In order to separate out different analytes, different eluents are used to

preferentially dissolve the analyte based on its polarity and other characteristics. There are many expensive machines which accomplish this, but we used the equipment available in the lab which allows us to perform the flash chromatography manually, using a column, an air pump, and a series of silica and sand filters. Figure 13 is an approximate description of the system.

Packing the Column

1. Pack the chromatography column with a small piece of wool, enough to fill the stopcock hole.
2. Add appx. 1cm of sand to the column.
3. In a small flask, mix silica beads with hexane, fill the column with about 10-15cm of this solution.
4. Use the air pump to compact the mix.
5. In a small flask, mix the BP dimer, dissolved in dichloromethane, with silica beads.
6. Add appx. 1 cm of sand to the top of the column.

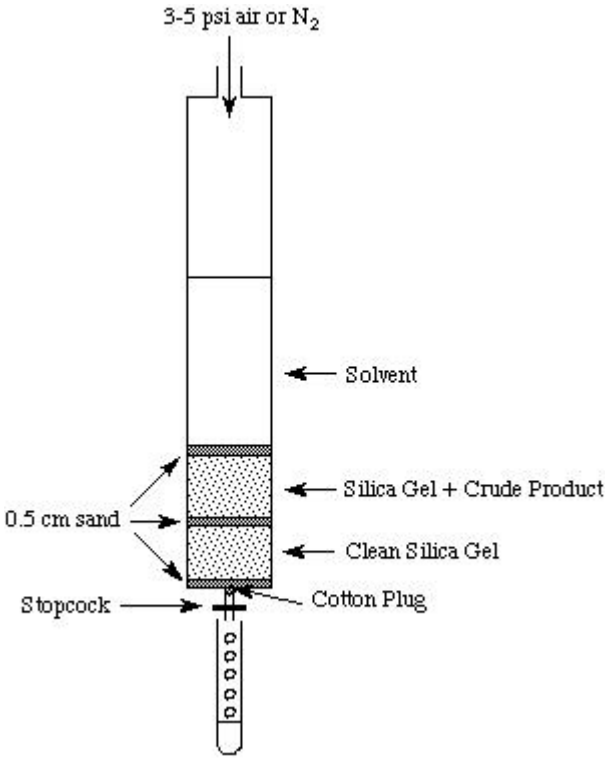

Figure 13: Flash Column Preparation [Scharrer 2013]

Separation Procedure

I diluted the sample with dichloromethane and then performed liquid column chromatography, using 100% hexane, then 50-50 hexane and ethyl acetate, and finally 100% ethyl acetate as eluents, to separate the solution into about 24 samples of approximately 20 mL (giving about 8 samples per eluent mixture). From these samples, I performed Thin Layer Chromatography (TLC). In TLC, a thin coating of some adsorbant material is layered

on a surface. The paper is then marked with a small amount of sample, and then placed in a beaker containing a few tens of mL of eluent at the bottom. The eluent is then allowed to climb up the paper, while constituents which are lighter and more soluble in the eluent will climb higher. This allows for dissemination between different kinds of products by their heights (Figure 14).

Figure 14: TLC Apparatus

Figure 15 is an example of my TLC results. In this example, see that successive samples tested have different products and were to be separated.

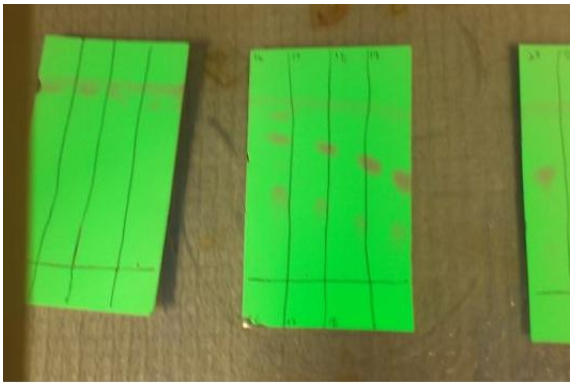

Figure 15: Left: This is an example of a good TLC result, in which successive samples can be group based on their heights. To the right we have an example of an inconclusive TLC result, in which the card was somehow tilted during the run, making it difficult to distinguish he relative heights.

After combining the samples based on which product they contained, we ran mass spectroscopy on each product to determine which contained the benzophenone dimer. After correctly identifying the dimer, the sample was destroyed by an accident in the lab. The process was then repeated with 100mg of benzophenone succinimide powder dissolved in 12 μL of 1,3-Diaminopropane. This sample was again sent in for mass spectroscopy as well as NMR analysis.

The mass spectroscopy data showed that we did create a symmetric benzophenone dimer shown by the 513.2 peak (Figure 16).

I used BioChemDraw to predict the NMR results of a pure benzophenone dimer. Given the NMR results, it was clear that, without further purification, it would be difficult to get conclusive results about the product. However, the mass spectroscopy results were strong enough evidence to move ahead

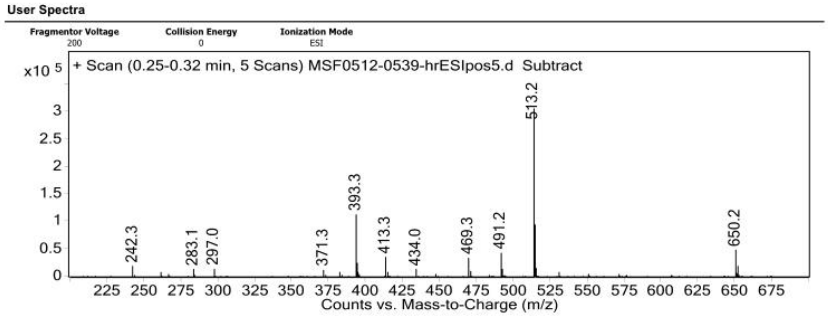

Figure 16: Mass Spectroscopy Results

and attempt fabrication with the new molecule.

2.2.3 Fabrication Solution

2mg of the benzophenone dimer was dissolved in 50 μL of dimethyl sulfoxide, 23 μL of polyethylene glycol diacrylate (455008, Sigma-Aldrich), and 320 μL of a HEPES buffer. The HEPES buffer is prepared from 20 mM (pH 7.3) HEPES (L6876, Sigma-Aldrich) and 100 mM NaCl. Lyophilized BSA (BAH-64, Equitech-Bio) was then added dry to the photosensitizer solution, yielding final weight percentages of 5% and10% for protein and DMSO, respectively.

2.3 Results and Discussion

The specific benzophenone dimer we created failed to act as a photosensitizer for proteins using the Ti:S laser, and we could not fabricate viable structures. There are several possible reasons. First of all, the benzophenone did not

dissolve well in the fabrication solutions we use in our lab. As soon as the saline buffer was added, the benzophenone dimer precipitated out and needed much centrifugation in order to dissolve. This dimer is much less rigid than benzophenone by itself; it is possible that the dimer absorbed a lot of the energy through vibrations rather than by forming C-H and C-C bonds. It may be that the molecular interactions between our benzophenone dimer and our protein solution has caused the dimer to not take on the specific conformation required for two photon absorption at the wavelengths we used. A much deeper analysis of the electronic and mechanical structure of our dimer is needed in order to fully understand why it did not work as a photosensitizer. In a broader sense, further research should focus on the molecular interaction between proteins and photosensitizers.

3 Trypsin Digestion of Bovine Serum Albumin

3.1 Theory and Motivations

Based on the benzophenone study, it became clear that the molecular interaction between the photosensitizer and the protein is very important for the ability to fabricate as well as the functional properties of the successive structures. One functional property of interest to the lab, as discussed earlier, is the swelling of structures due to changes in pH of the solution the

structures sit in. This swelling is assumed to be due to three phenomena: 1) deviation from the isoelectric point, leading to charge repulsion between protein molecules, 2) ion shielding of the charged centers of the protein structures due to salt concentrations or 3) temperature changes. The amount of swelling itself is assumed to be dependent on the density of crosslinking, which can be affected by the charge, size, and other molecular properties of the protein. In this study, I enzymatically digested a protein, bovine serum albumin, and used the resulting protein fragments for fabrication. I then compared the fabrication and swelling properties of the digested protein to the unperturbed form.

3.1.1 Isoelectric Point and Electrostatic Repulsion

The isoelectric point (pI) is the pH at which a molecule has no overall net charge. This occurs as relative concentrations of hydrogen ions run acid/base reactions forward and backwards about new, concentration-dependent equilibria. In reference to a protein, each amino acid has a number of amine or carboxyl groups with a specific acid dissociation constant (pKa), which constrains the relative concentrations of that acid or base and its neutral counterpart according to the following equation:

$$Ka = \frac{[A^-][H^+]}{AH} \tag{1}$$

and

$$pKa = -log[Ka] \tag{2}$$

with similar equations for bases. The ratio of the acid/base to its neutral counterpart is thus dependent on the concentration of hydrogen and hydroxide ions. The pI is the pH at which the concentration of hydrogen ions allows for the overall charge on the molecule to be neutral. The pI can be found experimentally by following migration of the protein in an electric field while varying pH. Upon deviations from the isoelectric point, the protein molecules in solution will be charged, and thus will repel each other allowing for swelling. This should occur with deviations to both sides of the pI, though some experiments in the lab have shown further shrinking at a pH below the pI, and this phenomena should be looked into further. In this experiment, we will look only at deviations above the pI of our target molecule.

Upon digestion of a large, globular protein such as bovine serum albumin (BSA), many changes can occur to the pI. Although the overall charge of BSA is negative, giving a pI of about 4.7, a large molecule like BSA should have many different positive and negative charge centers. Each fragment will now have its own pI which may compete with the other fragments. In theory, our new range of pI's should compete, contributing less to the swelling than in the case of a single protein species.

3.1.2 Ion Shielding and Debye Length

In a neutral solution, two charged centers on a molecule interact according to normal coulomb forces, with a $\frac{1}{r}$ dependence. When a salt is added to the solution, ions are attracted to these charge centers, therefore shielding the forces holding that charged molecule together. This hovering cloud of ions is called a **screening cloud**. Inside this screening cloud, charged centers can still feel each others' electrostatic forces. Outside of this cloud, that interaction is said to be screened. To model this interaction, I will follow (weakly) a derivation from Physical Biology of the Cell [Philips, 2009].

We will assume for simplification that the cloud is a step function, but these results can be expanded to exponential falloff. Consider that inside the cloud, there is a difference of charged ions...

$$\Delta c = c_+ - c_- \tag{3}$$

such that

$$c_+ = c_\infty + \frac{\Delta c}{2} \tag{4}$$

as can be seen in Figure 17.

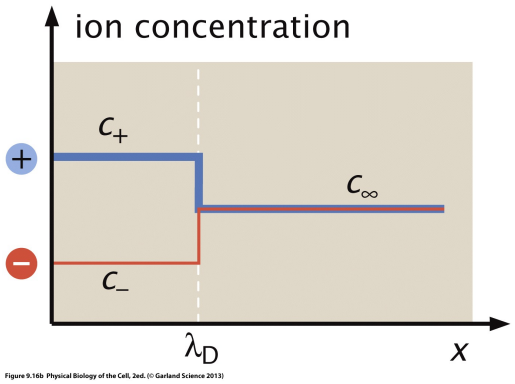

Figure 17: Concentration of Ions around a Charged Molecule [Philips, 2009]

The volume occupied by this screening cloud is just $A\lambda_D$ where A is the surface area of the molecule and λ_D is the length to which the screening length extends. Assuming the charges must cancel in order to shield the Coulomb interaction, the total charge in this screening cloud is $0 = Q_{molecule} - ze\Delta cA\lambda_D$.

Now we assume that the negative charge of the molecule sits at its surface, and that the positive charge of the screening ions is entirely distributed along the Debye surface, giving

$$E_{cloud} = \frac{Q}{\epsilon A} \tag{5}$$

where E is the electric field of the cloud, A is the surface area of the molecule, and ϵ is teh dielectric constant of teh medium. This gives the average potential of this cloud

$$V_{cloud} = -\frac{1}{2} E_{cloud} \lambda_D \tag{6}$$

where λD is the Debye length. The chemical potential outside the cloud is

$$\mu = \mu_0 + k_B T ln(\frac{c_\infty}{c_0}) \tag{7}$$

and the chemical potential inside the cloud is

$$\mu = \mu_0 + k_B T ln(\frac{c_\infty + \frac{\Delta c}{2}}{c_0}) + eV_{cloud} \tag{8}$$

where μ is the chemical potential, k_B is the Boltzmann constant, T is the temperature in Kelvin, and c is the concentration in mol/L. Setting these equal to each other and making the Taylor expansion $ln(1 + x) \approx x$, we find...

$$\lambda_D = \sqrt{\frac{\epsilon k_B T}{z^2 e^2 c_\infty}} \tag{9}$$

In this simplified model, we see that the charge and surface area of the molecule have canceled out along the way. Under general physiological conditions, where $\epsilon_{water} \approx 80\epsilon_0$ and $c_\infty \approx 100$mM, the Debye length is about 1nm.

In this study, we are looking at the percent change in Debye length with a change in pH. In this case, we are using buffer solutions, which include many

different kinds of salts at significant concentrations. The protein microstructures fabricated in the Shear lab can be thought of as randomly-crosslinked polymers with different, randomly distributed charge centers on the structure. By changing the pH and salt concentration, these charge centers which normally push the structure apart are shielded, causing the structure to shrink.

However, both of these effects (isoelectric point and ion shielding) may be counteracted if the density of crosslinking increases greatly by digestion of protein. With smaller fragments, it may be possible for both the fragments themselves and the free radicals created by the photosensitizer to diffuse more easily. During the fabrication reaction, we are creating a dense structure from a less dense one, meaning that constituents of the fabrication solution must in some way be pulled into the focal volume. One theory is that a lighter material will be more easily pulled into the focal volume to be crosslinked, leading to a higher density and therefore less swelling.

3.2 Experimental Design and Results

The digestion of bovine serum albumin with trypsin is a well-studied model system. Trypsin cleaves mainly at the C-terminal side of lysine and arginine except when next to a C-terminal proline. Due to these precise cuts, we can have an idea of how many, and what sized pieces we have after a certain amount of hydrolyzation of BSA by trypsin. The amino acid sequence can be found in the Protein Data Bank. In Figure 18 the lysines are highlighted in

green, the arginines are highlighted in purple, and the prolines are highlighted in yellow.

Figure 18: BSA Sequence

This gives the expectations for the total number of cuts, assuming 100% hydrolyzation.

Number of Amino Acids	Number C-Terminal Prolines	Number of Breakable Bonds
57 Arginines	3	54
22 Lysines	2	20
	Total Number of Breakable Bonds	74

To decide what amount of time to let the reaction run, we looked at previous papers [Qi, 2006] which had conducted hydrolyzation experiments of BSA by trypsin. Figure 19 shows the percent hydrolyzation (number of peptide bonds broken over the total number of bonds possible) plotted against the time the reaction ran. As we expect, the number of bonds increases

quickly at first, and then eventually slows.

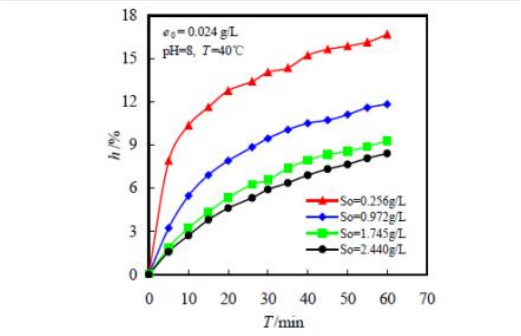

Fig. 2 Influence of substrate concentration on the degree of hydrolysis

Figure 19: Hydrolysis of BSA with Trypsin [Qi, 2006]

3.2.1 Reaction 1: Fabrication of Test Structures

Looking for a wide spread of hydrolyzation values in the smallest reaction time, we chose first to mimic the steepest curve. For an enzyme concentration of 24mg/L, the steepest slope is with the smallest BSA concentration tested, or 256mg/L.

4% hydrolysis $\approx$ 3 cuts

8% hydrolysis $\approx$ 6 cuts

12% hydrolysis $\approx$ 9 cuts

For the reaction, I titrated deionized water with NaOH to pH 8.0. I then added 0.256g/L BSA and allowed the BSA to dissolve over the stirring plate at 40C for one hour. I took out one fourth of this solution and added 0.024 g/L trypsin and 0.030mg/mL trypsin inhibitor to make the control sample.

Then, I added 0.024mg/mL trypsin to the rest of the protein solution, removing one fourth of the original mixture at the specified time intervals, adding 0.03mg/ml trypsin inhibitor at 2 min, 5.5min, and 16 min.

Once the trypsin inhibitor was added, the samples were flash-frozen in liquid nitrogen and placed on the lyophilizer until completely dry. Then, we used each of the samples to create a fabrication solution of 30% by weight BSA and 1% by weight rose bengal (Sigma Aldrich) dissolved in Hepes Buffer Solution (see Section 2.2.3 Fabrication Solution). In order to test the viability of the digested protein for fabrication, we put the solution through a series of fabrication image designs, each outlining a certain aspect of fabrication (i.e. ability to make circles, thin lines, and 3D features). They were then prepared for SEM. Results are seen in Figure 20, 21, and 22.

Preparation Protocol for SEM

1. Rinse 5X in HBS
2. Soak in 5% by weight gluteraldehyde in deionized water for 15 minutes.
3. Rinse 3X in deionized water and let soak for 15 minutes.
4. Rinse 3X in 1:1 deionized water and ethanol and let soak for 15 minutes.
5. Rinse 3X in ethanol and let soak for 15 minutes.
6. Rinse 3X in 1:1 ethanol and methanol and let soak for 15 minutes.
7. Rinse 3X in methanol and let soak for 15 minutes.
8. Place in desiccator for about 30 minutes or until completely dry.

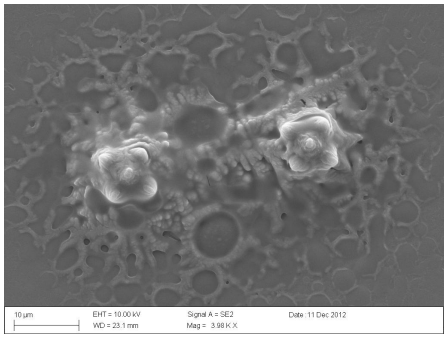

(a) Control

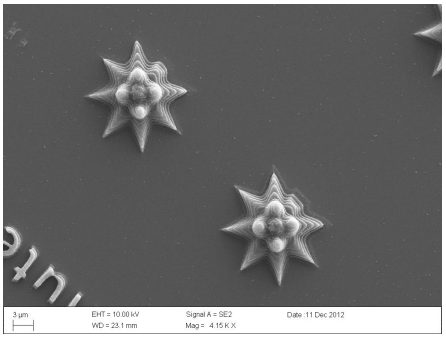

(b) 20 Min

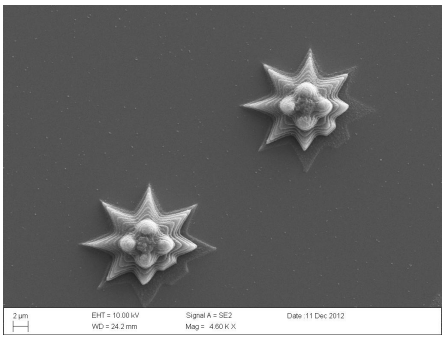

(c) 60 Min

Figure 20: SEM image of a 3-Dimensional Star. The control structures have some film deposited on them, perhaps because they weren't cleaned heavily enough before crosslinking. However, the 20 minute and 60 minute structures fabricated this structure very well. The 60 minute structures have a finer texture as suggested by thinner lines. This is most likely due to denser crosslinking and more efficient fabrication. However, it could also be due to the structure collapsing onto itself. Tilting the structures showed the latter not to be true.

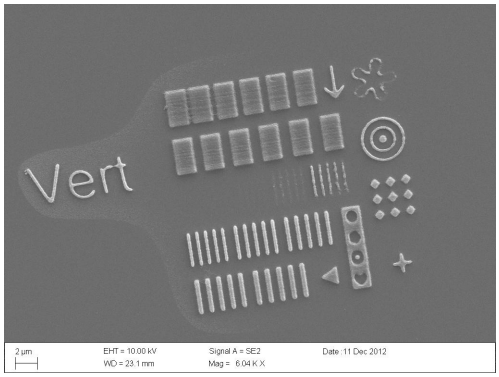

(a) Control

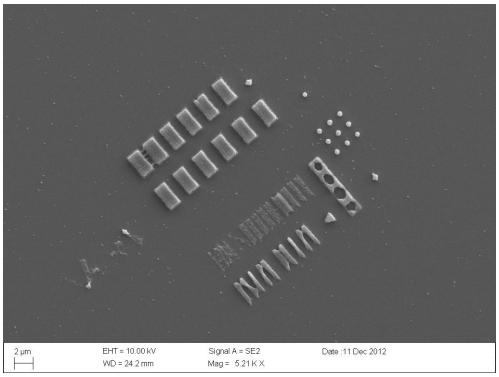

(b) 20 Min

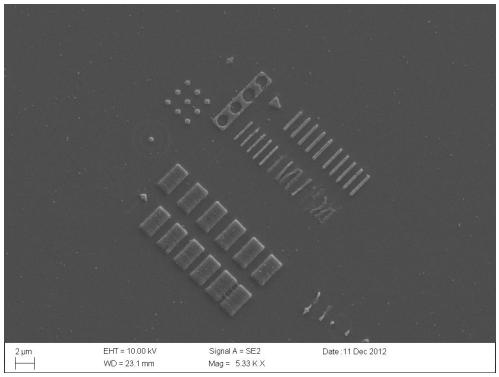

(c) 60 Min

Figure 21: Many smaller structures are intended to show accuracy and precision of the beam. Most noticeably, the control structure fabricated much more beautifully than either of the digested structures. Neither of the digested structures could handle circles or the thinnest row of lines, and are nearly identical in capability. However, the 20 minute structures are somehow swollen, likely due to less dense crosslinking. This made the 20 minute sample less able to produce the thinner lines.

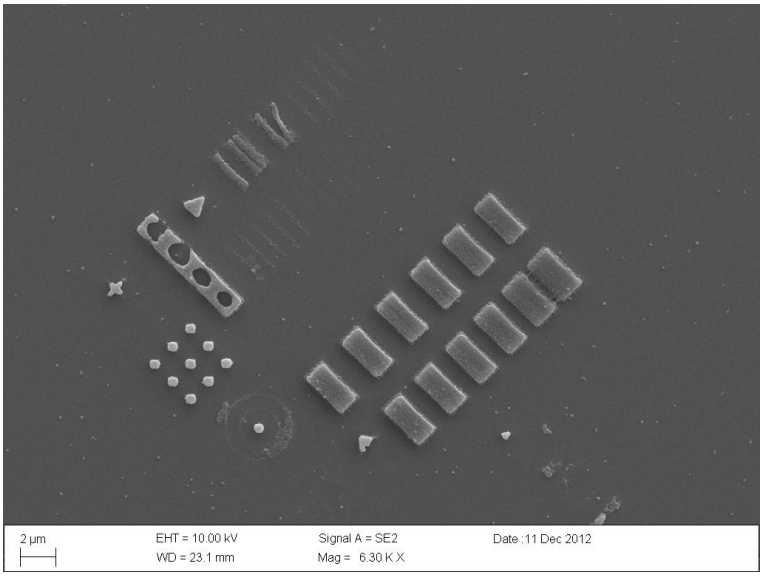

(a) 20 Min Horizontal Pattern

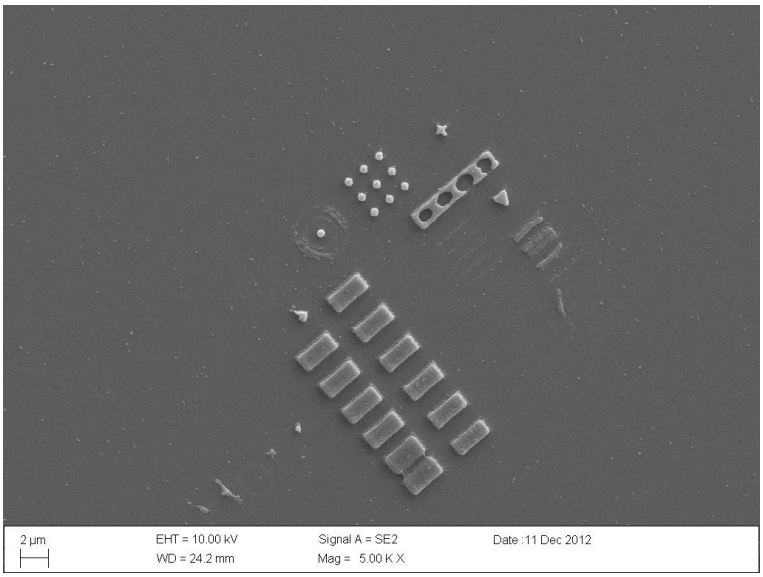

(b) 60 Min Horizontal Pattern

Figure 22: These are completely different structures than in the previous figure. These structures were fabricated under the same image, just rotated 90 degrees clockwise. This is to test whether the x or y direction on the fabrication machine has better precision. By turning the image, we can see that these samples can now produce circles, but can no longer produce thin lines. This tells us more about the fabrication machine than the structures themselves.

3.2.2 Reaction 1: Swelling Study

In order to test how the swelling properties changed due to digestion time, I used the digested protein to fabricate 10 μm x 10μm x 6μm square pads on #1 coverglass using the 100X/1.35NA oil immersion objective at a back-aperture power of 30mW. Solutions used for fabrication were 30% BSA and 1% rose bengal (Sigma Aldrich) by weight in HEPES buffer solution (see Section 2.2.3 Fabrication Solution). At the top corner of these squares, I fabricated a triangle which helped me focus the objective on the top of the pad during swelling. The structures were kept in a in a HEPES buffer at pH 7.3 and imaged using bright field microscopy. Then the structures were rinsed three times in a pH 4.7 20mM phosphate buffer and allowed to soak for two minutes before being imaged. The structured were then rinsed three times in the pH 7.3 HEPES buffer, rinsed again three times in the pH 9.0 20mM phosphate buffer, and then allowed to soak for two minutes in the pH 9.0 20mM phosphate buffer for two minutes before being imaged. Images look similar to those in Figure 23. Results are shown in Figure 24.

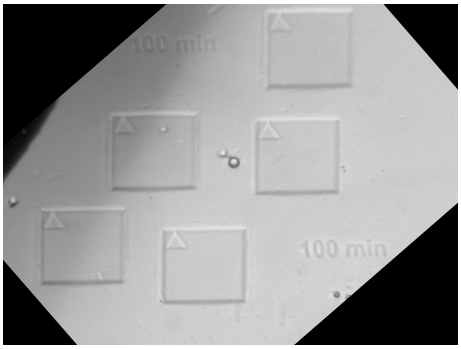

(a) pH 7.3

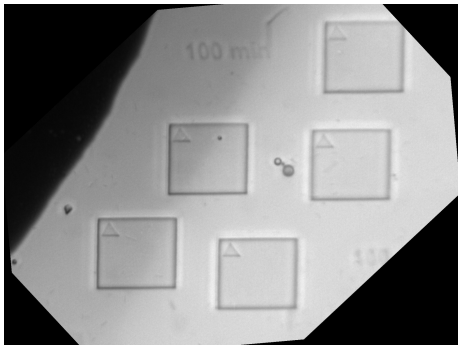

(b) pH 4.7

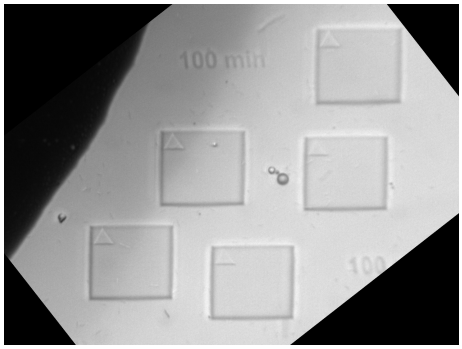

(c) pH 9.0

Figure 23: Here are examples of a typical swelling progression. At pH 7.3, the structures look normal compared to when they were fabricated. At pH 4.7, the top edges of the structure have migrated inward, leaving a shadow effect around the edges. At pH 9.0, the top is bulged, making it difficult to even focus on the triangle. The edges of the top portion of the structure are bulged out. In measuring these differences, the shading can often make it difficult to define exactly where the structure begins and ends.

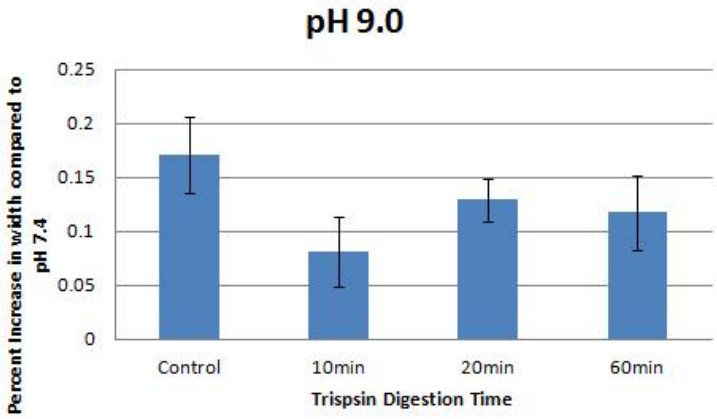

(a)

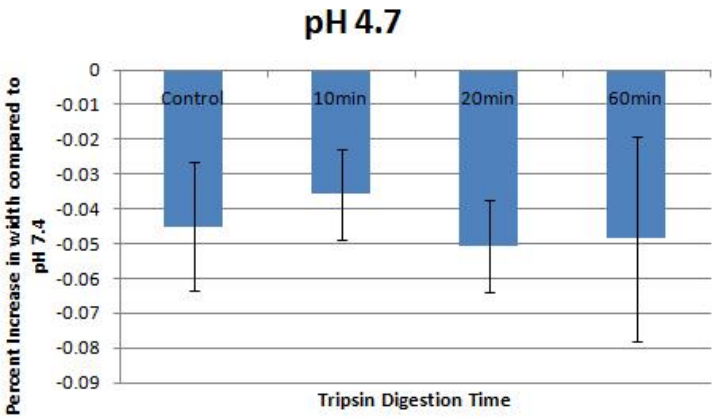

(b)

Figure 24: Shown are the percent swelling in the width of the pad in response to an added phosphate buffer solution of pH 9 (a) and contracting in responses to a phosphate buffer of pH 4.7 (b). Unfortunately, these changes in width are so small that the differences we see are within error of each other.

3.2.3 Reaction 2: Swelling Study

In seeing no significant changes in the swelling properties of the digested protein structures, we repeated the experiment. This time we used a wider range of digestion times, lasting up to 24 hours. Because we needed a high throughput of BSA, we chose the reaction with the highest concentration possible and proceeded to run the reaction in accordance to the methods given in the paper. Thus we ran the reaction at ten times the concentration of protein, 2.44g/L BSA, and the same concentration of enzyme, 0.024g/L trypsin and 0.030g/L trypsin inhibitor. Results are shown in Figure 25.

30 min = 5.5% hydrolysis $\approx$ 4 cuts

100 min = 10% hydrolysis $\approx$ 8 cuts

1 day = Unknown

1 week = Unknown

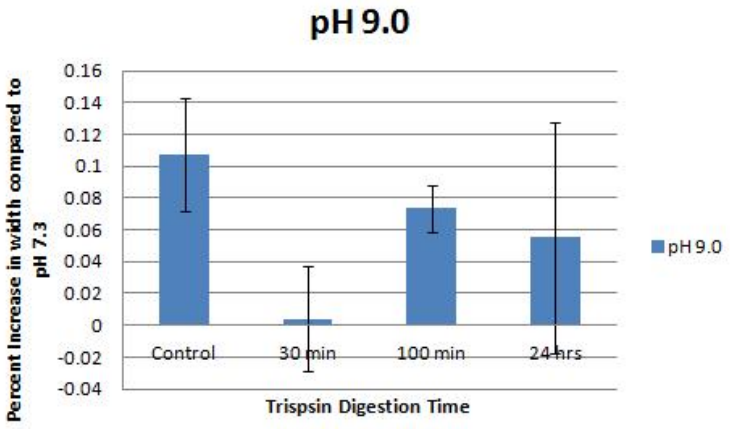

(a)

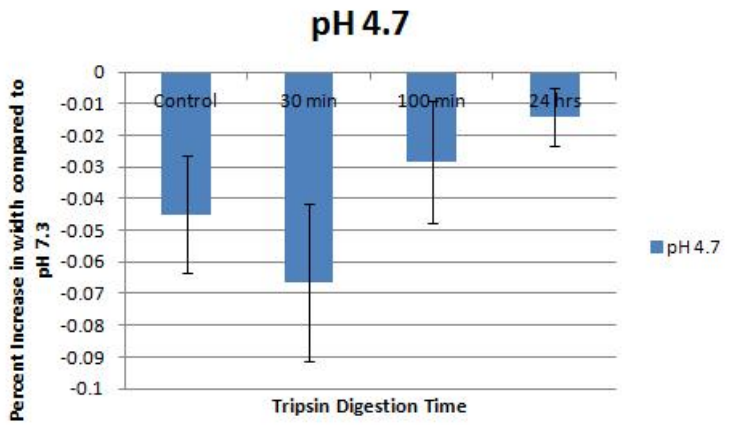

(b)

Figure 25: Shown are the percent swelling in the width of the pad in response to an added buffer of pH 9 (a) and contracting in responses to a buffer of pH 4.7 (b). Unfortunately, these changes in width are so small that the differences we see are again within error of each other.

3.3 Conclusion

From the SEM studies, we can see that the protein fragments were not as efficient for crosslinking small, thin, intricate structures. This could be due to many reasons, such as less dense crosslinking or some unidentified advantage of the BSA's large globular structure. For instance, many of the BSA residues are not able to crosslink, and it is likely that some of the digested fragments do not contain residues which will crosslink. However, the undigested protein was able to fabricate large three dimensional structures. In general, we can conclude from these results that the size and homogeneity of the "monomers" of our structures is only important when trying to fabricate small, intricate designs.

With respect to the swelling studies, we saw that there was little difference in swelling between the undigested and digested protein structures, even after letting the reaction run for 24 hours. Without seeing much of a change, it is difficult to continue the study or rule out any one variable. In order to find significance, further studies into finding the isoelectric point of the digested protein fragments are necessary. Quantization of the number, size, and charge of the specific protein fragments from our digestion, which would require further purification, mass spectroscopy, and NMR studies are necessary in order to further narrow down the possible effect of protein digestion on success in fabrication. Unfortunately, the cost of time and money to purify and identify the products would make the method unmanageable for daily use in fabrication. Alternatively, studies on fabrication with polymers

of different number and size of monomer would further clarify the effect of molecule size on fabrication.

References

[1] Connell, Jodi L., et al. "Probing prokaryotic social behaviors with bacterial "lobster traps." MBio 1.4 (2010).

[2] Connell, Jodi L., "Characterization and Microfabrication of Environmentally Sensitive Materials for Studying Bacterial Group Behaviors." (2012).

[3] Dorkenoo, Kokou D. Honorat, et al. "Monitoring the Contractile Properties of Optically Patterned Liquid Crystal Based Elastomers." (2012).

[4] Dorman, Gyorgy, and Glenn D. Prestwich. "Benzophenone photophores in biochemistry." Biochemistry 33.19 (1994): 5661-5673.

[5] Nielson, Rex, Bryan Kaehr, and Jason B. Shear. "Microreplication and Design of Biological Architectures Using Dynamic-Mask Multiphoton Lithography." Small 5.1 (2009): 120-125.

[6] Oliva, Brittany and Barron, Andrew. "Basics of UV-Visible Spectroscopy." Connexions. Web. 5 May 2013. `http://cnx.org/content/m34525/latest/`.

[7] Philips, Kondev, and Theroit. "Physical Biology of the Cell." (2009).

[8] Pitts, Jonathan D., et al. "New Photoactivators for Multiphoton Excited Three-dimensional Submicron Cross-linking of Proteins: Bovine Serum Albumin and Type 1 Collagen." Photochemistry and photobiology 76.2 (2002): 135-144.

[9] Prahl, Scott. "Optical Absorption of Methylene Blue." Oregon Medical Laser Center. Web. 5 May 2013. http://en.wikipedia.org/wiki/File:Methylene_blue_absorption_spectrum.png.

[10] Ritschdorff, Eric T., Rex Nielson, and Jason B. Shear. "Multi-focal multiphoton lithography." Lab on a Chip 12.5 (2012): 867-871.

[11] Scharrer, Eric. "Hydrolytic Kinetic Resolution of an Epoxide Using Jacobsen's Salen(Co) Catalyst – Purification by Flash Chromatography." Web. (May 5 2013). http://www2.ups.edu/faculty/escharrer/week11.htm.

[12] Shear, Jason B. "Peer Reviewed: Multiphoton-Excited Fluorescence in Bioanalytical Chemistry." Analytical chemistry 71.17 (1999): 598A-605A.

[13] Spivey, Eric C., et al. "Multiphoton Lithography of Unconstrained Three-Dimensional Protein Microstructures." Advanced Functional Materials 23.3 (2013): 333-339.

[14] Qi, Wei, and Zhimin He. "Enzymatic hydrolysis of protein: Mechanism and kinetic model." Frontiers of Chemistry in China 1.3 (2006): 308-314.

[15] Wang, Jun, et al. "Nonlinear optical properties of graphene and carbon nanotube composites." (2011).